SAND76-8663
Unlimited Release

Optical and Thermal Characteristics of a Solar Collector With a Stationary Spherical Reflector and a Tracking Absorber

(Presented at Society of Photo-Optical Instrumentation Engineers Annual Technical Symposium in San Diego, CA, August 23-27, 1976, and published in Proceedings Volume 85)

A. M. Clausing

Prepared by Sandia Laboratories, Albuquerque, New Mexico 87115 and Livermore, California 94550 for the United States Energy Research and Development Administration under Contract AT (29-1)-789

Printed August 1976

Sandia Laboratories
energy report

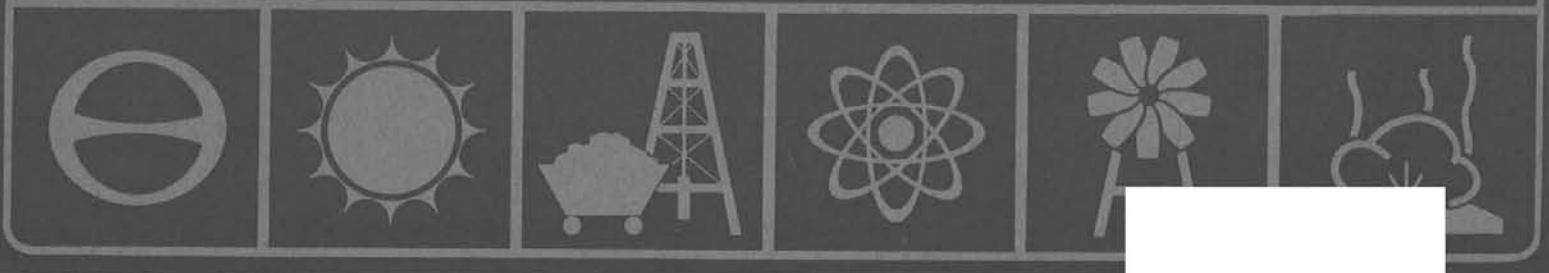

SF 2900-QQB(3-74)

Issued by Sandia Laboratories, operated for the United States Energy Research and Development Administration by Sandia Corporation.

OPTICAL AND THERMAL CHARACTERISTICS OF A SOLAR COLLECTOR WITH A STATIONARY SPHERICAL REFLECTOR AND A TRACKING ABSORBER

A. M. Clausing
Faculty Sabbatical Professor*
Solar Energy Technology Division 8184
Sandia Laboratories
Livermore, California 94550

Abstract

A fixed segment of a concave spherical mirror can be used to concentrate beam radiation onto a tracking absorber which pivots about the center of curvature of the mirror. A possible economic advantage of this solar collector over concentrating collectors with tracking mirrors is reduced mirror cost. The objective of the investigation is to determine the potential of this system for electrical power production. Special emphasis is given to identifying the penalty associated with the fixed reflector. The results showed appreciable cosine losses even at the best times of the year. The overall system efficiency was found to be strongly dependent on the rim angle, the optical efficiency, the absorber temperature, and the degree of selectivity of the absorber surface.

Introduction

A stationary, concave, spherical reflector would focus parallel light essentially at a point if the radius of the aperture of the mirror R_a were much less than its radius of curvature R_S. In the proposed collector, R_a is of the same magnitude as R_S; hence, the focus becomes blurred due to spherical aberration. For example, parallel rays perpendicular to the aperture of a hemispherical mirror are focused along a line which extends from the mirror's surface to $R_S/2$ as illustrated in Figure 1. Hence, an absorber which is to intercept all of the specularly reflected energy from such a mirror must have a length of approximately $R_S/2$. Furthermore, since the proposed system has a fixed mirror, the absorber must be pivoted about the center of curvature and track the sun in order to be kept at the line focus (see Figure 2).

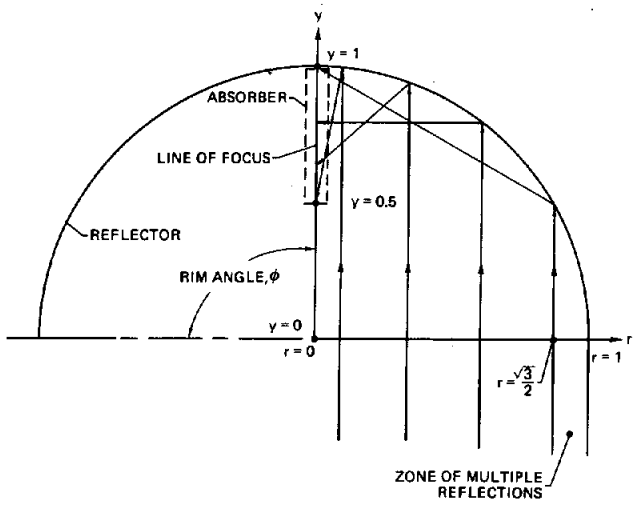

Fig. 1. Ray Pattern for Spherical Mirror With Rays Perpendicular to Plane of Aperture

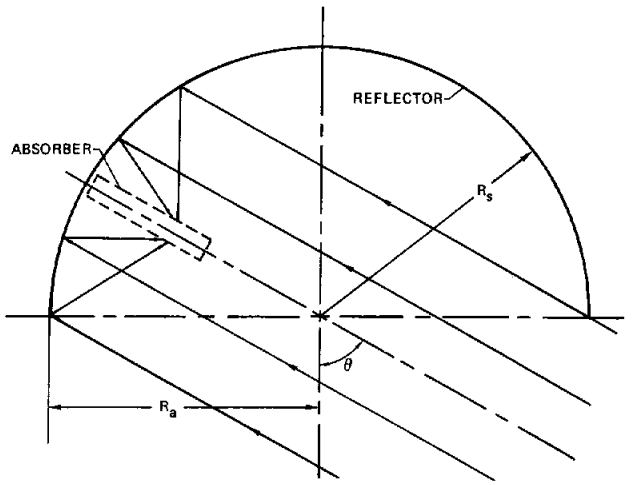

Fig. 2. Reflecting Characteristics of Spherical Mirror With Rays at Angle of Incidence θ

The main advantage of the SRTA collector is the fixed mirror. It enables the construction of extremely large units without prohibitive costs. Large collectors, in turn, result in greatly reduced transport losses or in significantly fewer converters if one is used in conjunction with each collector. A major disadvantage of the SRTA collector is the cosine loss. This loss is due to the fact that the direct solar radiation incident on the aperture of the collector is proportional to the cosine of the angle of incidence; i.e., the angle between the sun's rays and the normal to the plane of the aperture. The cosine loss is common to all collectors that do not track the sun.

* Associate Professor of Mechanical Engineering, University of Illinois, Urbana, IL 61820

The SRTA collector was first described by Steward,[1] who gave a brief description of the system. Steward and Kreith[2] recently published a more complete description including an analysis of the axial variation of the concentration ratio; however, they did not consider the overall performance characteristics of the system. Kreider[3] analyzed the thermal performance of the SRTA collector, but his study did not include the diurnal or yearly variations.

The objective of this study is to determine the potential of the SRTA collector for electrical power production and to clearly establish its optical and thermal performance characteristics. Special emphasis is given to identifying the penalty associated with the fixed reflector.

Optical Characteristics of Collector

It is convenient in describing the effectiveness of SRTA concentrators to introduce a nominal concentration ratio which is defined as the ratio of the aperture area to the receiver area*

$$CR \equiv \frac{A_a}{A_r} \tag{1}$$

Also, the nominal hemispherical concentration ratio is, by definition

$$CR_H \equiv \frac{\pi R_s^2}{A_r} \tag{2}$$

The usefulness of CR_H is not restricted to hemispheres. However, if the rim angle ϕ is 90°, $CR_H = CR$, hence the name nominal hemispherical concentration ratio. The minimum area of the receiver which is required to intercept the complete image of the sun is desired in order to obtain an upper bound for these concentration ratios.

Consider the image of the sun with perfect optics when the rays are perpendicular to the plane of the aperture as shown in Figure 1.** The coordinates, which are normalized with respect to the radius of curvature R_s, are also shown. The rays passing through the aperture near $r = 0$ intercept the axis near $y = 0.5$; the ray passing through $r = \sqrt{3/2}$ intercepts the axis at $y = 1$; and all rays with $r > \sqrt{3/2}$ experience multiple reflections. The number of reflections, n, experienced by a ray before it passes through the axis of the mirror is

$$n = \left[\frac{\theta}{\pi - 2\theta}\right]^{\dagger} + 1 \tag{3}$$

where θ is the angle of incidence of the ray on the reflector. It can be shown from the geometry depicted in Figure 1 that

$$\theta = \sin^{-1} r \tag{4}$$

It also follows that the location of the point of intersection of the ray with the y-axis is

$$y = \frac{r}{(-1)^{n-1} \sin(2n\theta)} \tag{5}$$

and the distance D the ray travels before intercepting the y-axis after n reflections is:

$$D = (n-1)\frac{\sin(\pi - 2\theta)}{\sin\theta} + \frac{\sin[(2n-1)\theta]}{\sin(2n\theta)} \tag{6}$$

* An external non-cavity receiver geometry is assumed. The areas of the ends of the receiver are assumed to be perfectly insulated and are not included in the definition of A_r.

** The diffuse energy collected by the SRTA collector is generally negligible; therefore, it is ignored in all definitions and analyses.

† [x] denotes the greatest integer not greater than x.

Since the local radius of the receiver is much less than the radius of curvature of the mirror, Eq. (6) provides a good approximation for the distance the ray travels after its first reflection before it intercepts the absorber. The absorber diameter which is required to intercept the entire image of the sun with perfect optics and perfect tracking is dependent on this distance and the angle substended by the sun. The angle substended by the sun at mean sun-earth distance is 0.0093 radians.

Consider first the case of a rim angle of 60°; therefore, no multiple reflections occur with the collector-sun orientation shown in Figure 1. The required absorber diameter for this case at mean earth-sun distance varies linearly from 0.0046 R_S at y = 0.5 to 0.0093 R_S at y = 1; hence, the theoretical maximum nominal hemispherical concentration ratio is 288. A 90° rim angle requires a wider absorber in the region y > 0.92 in order to account for the longer path lengths traveled by the multiply reflected rays. The required absorber diameter varies from 0.0046 R_S at y = 0.5 to 0.0146 R_S at y = 1. The variation is linear only from y = 0.5 to y = 0.92. The required increase in receiver area results in a theoretical maximum nominal hemispherical concentration ratio of 270.

Although a rim angle of 60° results in no multiple reflections when the rays are normal to the aperture, multiple reflections still occur at all other angles of incidence. More generally, if the rim angle is greater than 45° and if the collector is to be utilized when the angle of incidence is greater than 45°, the minimum value of A_r is independent of rim angle and is a function only of the radius of curvature of the mirror. The theoretical maximum nominal hemispherical concentration ratio is a constant, 270. Since the mirror accuracy and tracking accuracy should also be relatively independent of rim angle, it follows that

$$CR \simeq CR_H \sin^2 \phi \tag{7}$$

Likewise, the effective concentration ratio, which is defined as the ratio of the area of the aperture projected in a plane normal to the rays of the sun to the area of the receiver, is

$$CR_e \simeq CR_H \sin^2 \phi \cos \theta \tag{8}$$

The influence of the rim angle and the angle of incidence on the effective concentration ratio is given in Table I which clearly shows the disadvantage of small rim angles.

Table I

Influence of Angle of Incidence and Rim Angle on the Effective Concentration Ratio (CR_e/CR_H)

ϕ \ θ	0°	15°	30°	45°	60°	75°
90°	1.00	0.97	0.87	0.71	0.50	0.26
75°	0.93	0.90	0.81	0.66	0.47	0.24
60°	0.75	0.72	0.65	0.53	0.38	0.19
45°	0.50	0.48	0.43	0.35	0.25	0.13

The relatively large receiver required in the SRTA collector may be partially offset in some applications by the nonuniform energy distribution along the "line" focus. For example, if a constant diameter, circular cylinder is used as the absorber with a reflector having a 60° rim angle, the ratio of the local heat flux on the receiver q_r to the average $\bar{q}_r$ when the sun's rays are normal to the aperture is

$$\frac{q_r}{\bar{q}_r} = \frac{4}{3} r \frac{dr}{dy} = \frac{1}{3y^3}, \quad 0.5 \le y \le 1 \tag{9}$$

where dr/dy was eliminated by using Eq. (5) with n set equal to one. The flux at y = 0.5, 0.75, and 1.0 is 2.67 $\bar{q}_r$, 0.79 $\bar{q}_r$, and 0.33 $\bar{q}_r$, respectively. Unfortunately, the heat flux distribution is a function of the angle of incidence; hence, it is dependent on both the time of the year and the time of the day. A strong circumferential variation in the flux distribution arises whenever θ is large. Designing an optimum receiver for the SRTA collector system for these reasons is probably a more difficult task than for any other collector system.

The influence of the angle of incidence on the effective concentration ratio has been established. The diurnal and yearly variation of this angle and the influence of aperture slope remain to be described. Simultaneously, a more important question can be addressed--the determination of the cosine loss. Since the solar intensity is nearly flat over a sizable portion of the day, the cosine of the angle of incidence averaged over the day (the average daily cosine) and further averaged over the year (the average yearly cosine) give indications of the fraction of energy lost with a fixed reflector or with a single axis of tracking.

It will be assumed that the aperture azimuth angle (the angle measured in the horizontal plane from south to the horizontal projection of the normal to the aperture) is zero. The tilt or slope of the collector S is defined as the angle between the rear face of the plane of the aperture and the horizontal plane. The optimum slope is to be determined. It is not difficult to show that the cosine of the angle of incidence is

$$\cos\theta = \sin d \sin(\ell - S) + \cos d \cos h \cos(\ell - S) \quad , \quad |h| < h_{ss} \tag{10}$$

where d is the sun's declination, ℓ is the latitude, h is the hour angle, and h_{ss} is the hour angle at sunset. Equation (10) shows that the angle of incidence is a function only of the declination, the hour angle, and the difference between the latitude and slope (ℓ - S). If S is equal to ℓ, Eq. (10) reduces to

$$\cos\theta = \cos d \cos h, \quad S = \ell \tag{11}$$

The diurnal variations of the cos θ at summer solstice, equinox, and winter solstice are given in Figures 3 and 4 for (ℓ - S) equal to 35° and 0°, respectively. Figure 3 shows the poor winter performance which is typical for horizontal collectors at latitudes within the Continental United States. On the other hand, Eq. (11) and Figure 4 both show that if atmospheric attenuation is neglected, a collector with ℓ = S performs as well during sunlit hours at winter solstice as it does at summer solstice.

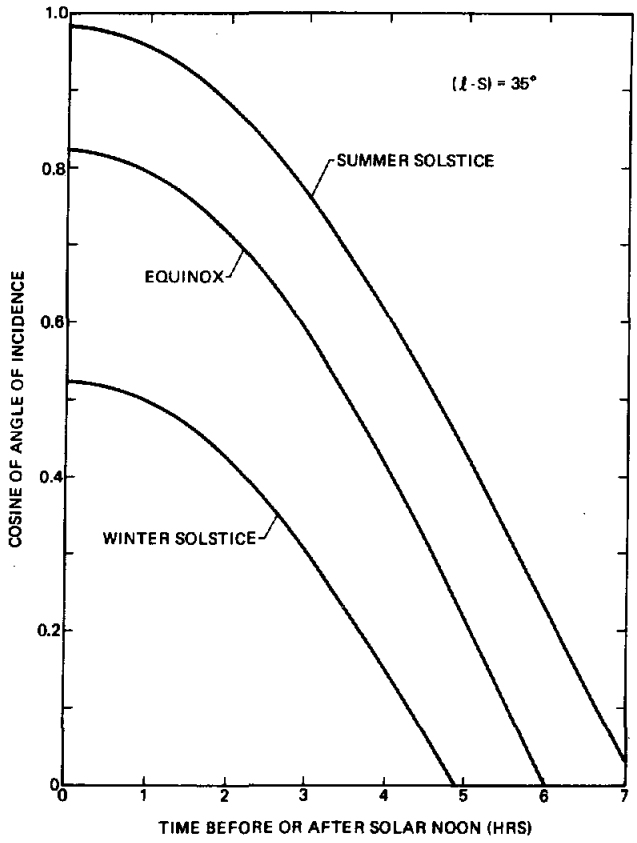

Fig. 3. Cosine of Angle of Incidence Versus Time of Day, (ℓ - S) = 35°

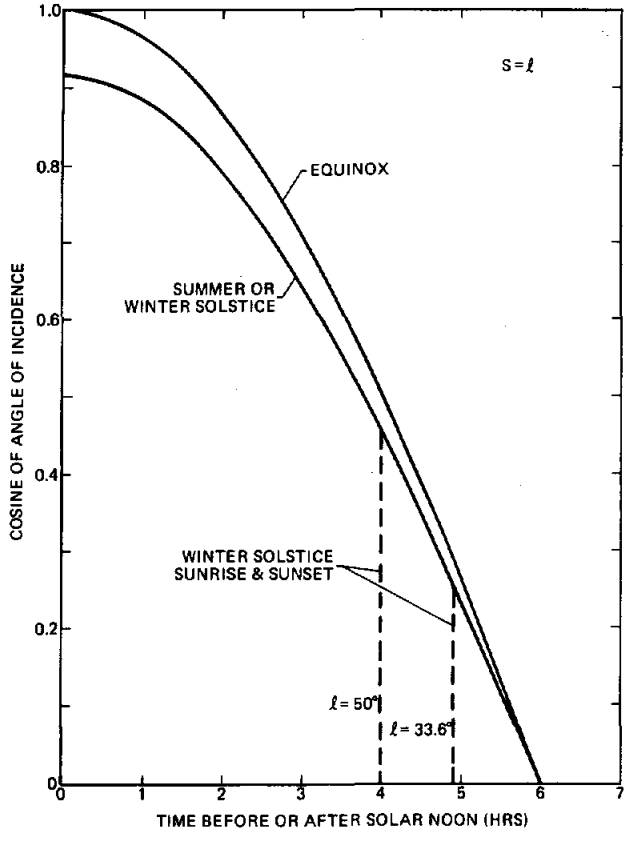

Fig. 4. Cosine of Angle of Incidence Versus Time of Day With Aperture Slope Equal to Latitude

The average daily cosine is desired in order to determine the fraction of the available energy which is intercepted by a collector with a fixed mirror. A collection period centered about solar noon of length 2 t_f is of interest. The average daily cosine is

$$\overline{\cos\theta}\,|_{day} = \frac{1}{t_f}\int_0^{t_f} \cos\theta \; dt \tag{12}$$

where the time t is measured from solar noon. If Eq. (10) is substituted into Eq. (12) and the small variation in the sun's declination throughout the day is neglected, one obtains

$$\overline{\cos\theta}\,|_{day} = \sin d \sin(\ell - S) + \cos d \cos(\ell - S)\frac{\sin h_f}{h_f}, \quad h_f > h_{ss} \tag{13}$$

The variation of the average daily cosine with the time of the year is shown in Figure 5. The poor performance from autumnal equinox through vernal equinox for collectors with large values of $(\ell - S)$ is clearly shown. On the other hand, a variation of only ±4.3 percent occurs in the average daily cosine if $(\ell - S)$ is zero.

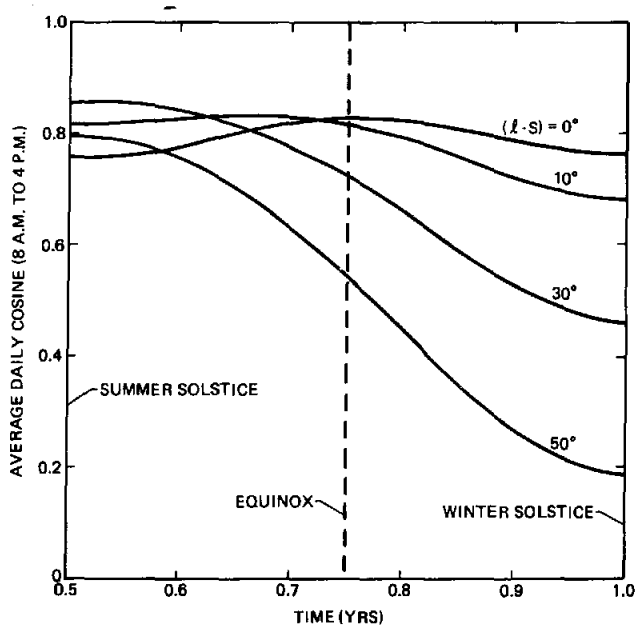

Fig. 5. Average Daily Cosine (8 a.m. to 4 p.m.) Versus Time of Year

If the average daily cosine is integrated over the year, an indication of the influence of day length and collector slope on the total yearly output of the collector is obtained. The yearly average cosine is defined as

$$\overline{\cos\theta}\,|_{yr} = (yr)^{-1}\int_0^{1\,yr} \overline{\cos\theta}\,|_{day}\; dt \tag{14}$$

where t is the time in years. If Eq. (13) is substituted into Eq. (14), one obtains

$$\overline{\cos\theta}\,|_{yr} = 0.0067 \sin(\ell - S) + 0.9592\frac{\cos(\ell - S)\sin h_f}{h_f}, \quad h_f > h_{ss} \tag{15}$$

The sun's declination used in the determination of the numerical coefficients in Eq. (15) was obtained from the 1977 Ephemeris[4]; the ASHRAE approximation for the sun's declination[5] gave 0.0059 and 0.9593, a negligible difference. The average yearly cosine is based on a fixed length day; a more meaningful but less convenient criterion for the termination of the integration would be a minimum level of insolation on the collector aperture. Since the average daily cosine is a strong function of the time of the year only for large values of $(\ell - S)$, the two criteria will give similar results when $(\ell - S)$ is small. Since the $\cos(\ell - S)$ is an even function and since the coefficient of the $\sin(\ell - S)$ is small, the value of $(\ell - S)$ which results in the maximum average yearly cosine is approximately zero for all day lengths, and the sign of $(\ell - S)$ has a minor influence on $\overline{\cos\theta}\,|_{yr}$.

The evaluation of collector performance is greatly simplified using Eq. (15) since it enables the calculation of average yearly cosines at any latitude for any collector slope and applicable day length without performing any numerical integrations. It should be remembered, however, that the average yearly cosine does not include the influence of daily or yearly variations in the attenuation of the beam radiation by the atmosphere. These variations stem from: (a) changes in atmospheric path length, (b) dust, smog, or moisture, and (c) cloud cover. The influences of the day length and aperture slope on the average yearly cosine are shown in Figure 6. The restriction $h_f > h_{ss}$ means that the maximum latitudes at which these results can be applied are 63.4°, 58.5°, 49.1°, 30.8°, and 0° for day lengths of 4, 6, 8, 10, and 12 hours, respectively.

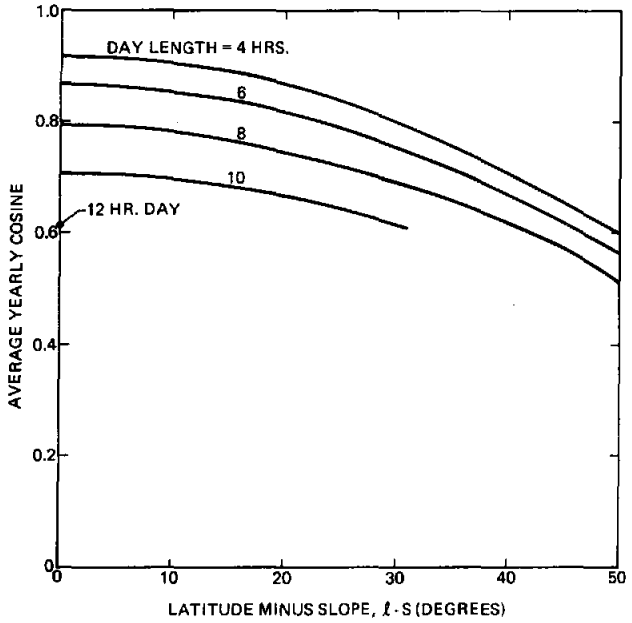

Fig. 6. The Influence of Day Length and Aperture Slope on the Average Yearly Cosine

Model of SRTA Collector System

The potential of the SRTA collector system for electrical power production is to be determined. The following assumptions and conditions are employed in the model which is used in the evaluation.

(i) A clear day and the validity of a modified ASHRAE model for the calculation of direct insolation are assumed. Specifically, the expression used for the direct normal insolation I_{dn} is:

$$I_{dn} = CN \cdot f_1(\text{day}) \cdot \exp\left\{\frac{-f_2(\text{day}) \cdot (1 + C_1/\cos\psi_o)}{\cos\psi + C_1}\right\} \qquad (16)$$

where CN is the clearness number, ψ is the sun's zenith angle, ψ_0 is the zenith angle at solar noon, f_1 and f_2 are prescribed functions of the day of the year, and C_1 is an empirical constant. The basis for this equation and comparisons with experimental data from Goldstone and Inyokern, CA are given in Reference 6. A clearness number of 1.0 was used throughout the year, and 0.2 was used for the constant C_1.

(ii) An isothermal absorber was used in the analysis. In practice, the receiver would probably not be isothermal; however, a more realistic description requires specification of heat transfer fluids used in the absorber, the parameters of the thermal cycle, etc. In addition, temperature drops occur: (a) between the surface of the receiver and the heat transfer fluid used in the absorber, (b) along the piping which transports the thermal energy from the receiver to the thermal engine or the heat exchanger if an intermediate loop is used, and (c) in intermediate heat exchangers if required. All heat losses other than convective and radiative losses from the receiver surface were neglected. Also, the heat losses from the ends of the receiver were neglected. The heat loss with an isothermal receiver is not expected to exceed the total loss from a nonisothermal receiver which delivers a working fluid to the thermal engine at the assumed receiver temperature T_r.

(iii) The efficiency of the thermal engine which is used to convert the thermal energy to electrical energy was assumed to be equal to the Carnot efficiency, which is

$$\eta_c = 1 - \frac{T_{sink}}{T_r} \tag{17}$$

Since no engine operating between two given temperatures can be more efficient than a Carnot engine operating between the same two temperatures, the use of this efficiency provides an upper bound of the electrical power produced.

(iv) The absorber was assumed to be semi-gray with a solar absorptance α and an infrared emittance ϵ. The surroundings were assumed to be black (by virtue of geometry) at a uniform temperature T_s. The analysis is valid for any receiver shape as long as the view factor of the receiver with itself is small. The absorptance was assumed to be independent of the angle of incidence.

(v) The absence of a cover plate over the absorber surface was assumed in the calculation of the convective heat loss. Since the heat transfer coefficient due to natural convection in air is nearly independent of ΔT for the conditions of this study (in fact, the Grashof number actually decreases slightly with increasing absorber temperature), the convective heat exchange between the absorber and the ambient air at temperature T_a was based on a constant heat transfer coefficient of 8 W/m^2 - K (1.4 BTU/hr - ft^2 - °F).

(vi) The specular reflectance ρ of the mirror was assumed to be independent of wavelength and angle of incidence. It was further assumed that all rays undergo a single reflective loss. The maximum percent of the energy which can undergo two or more reflections is 25 percent. The effect of multiple reflections could be partially accounted for by an artificial reduction in the reflectance.

(vii) The approximation for the sun's declination proposed by ASHRAE[5] is used. The latitude was assumed to be 33.6 degrees.

The heat loss Q_L from the receiver with the simplifying assumptions which are stated is

$$Q_L = hA_r(T_r - T_a) + \sigma\epsilon A_r(T_r^4 - T_s^4) \tag{18}$$

where h is the average convective heat transfer coefficient, A_r is the area of the receiver, and σ is the Stefan-Boltzmann constant. The incident solar energy absorbed by the receiver is

$$Q = A_a(\delta\rho\gamma\tau\alpha) I_{dn} \cos\theta \tag{19}$$

or

$$Q = A_r(CR)\eta_0 I_{dn} \cos\theta \tag{20}$$

where I_{dn} is the direct normal insolation, θ is the angle of incidence, and η_0 is the optical efficiency. Optical losses common to SRTA collectors are: blocking losses, reflection loss, intercept losses, transmission losses, and absorption losses. The absorber, tracking boom, and support struts shade the reflector; hence, only the fraction δ of the energy incident on an identically orientated bare reflector reaches the actual reflector. A specular reflectance ρ less than unity accounts for the reflection loss. Only the fraction γ of the specularly reflected energy is intercepted by the absorber due to imperfect optics and tracking, and blockage by system components. If a cover plate is used, only the fraction τ of the intercepted energy is transmitted through the cover plate. Finally, only the fraction α of the energy incident on the absorber is absorbed. The optical efficiency η_0 is the product of these five fractions--$\delta\rho\gamma\tau\alpha$. The self-shading of the reflector is excluded from the optical losses; this loss is implicit in the cosine loss.

A meaningful barometer of the performance of the collector system is the overall system daily efficiency η which is defined as

$$\eta = 100 \frac{\int_0^{t_f} (Q - Q_L)\eta_c \, dt}{\int_0^{t_{ss}} I_{dn} A_a \, dt} \tag{21}$$

where t = 0 corresponds to solar noon, t_{ss} the time from solar noon to sunset, and t_f is the time at which the net thermal output of the collector $(Q - Q_L)$ becomes negative. The overall system daily efficiency is 100 times the daily energy output of the engine divided by the total energy incident on a tracking plane surface of area A_a.

Results

A set of representative parameters were chosen as the standard case in order to facilitate comparisons in the parametrical investigations. Specifically: a rim angle ϕ of 90°, a nominal hemispherical concentration ratio of 100, a slope S of 34°, an emittance ϵ of 0.22, an optical efficiency η_0 of 0.76, a time of the year of vernal equinox, an absorber temperature T_r of 500°C (932°F), an ambient temperature T_a and a temperature for the surroundings T_s of 20°C (68°F), and a sink temperature T_{sink} of 40°C (104°F). Only those parameters which differ from the standard set are specified in the figures.

A comparison between the diurnal variations in the collector instantaneous output and the direct normal insolation is given in Figure 7. The direct normal insolation and the collector output are both normalized with respect to their respective values at solar noon. The direct normal insolation predicted by the model as well as experimental data from a clear day near vernal equinox at Inyokern, California, are provided. The model and experimental data agree well and show high values of the direct normal insolation throughout the day with an attenuation of less than 25 percent at one hour before sunset or after sunrise. In contrast, the SRTA collector output is sharply peaked and is attenuated by more than 50 percent at 2-1/2 hours before sunset or after sunrise.

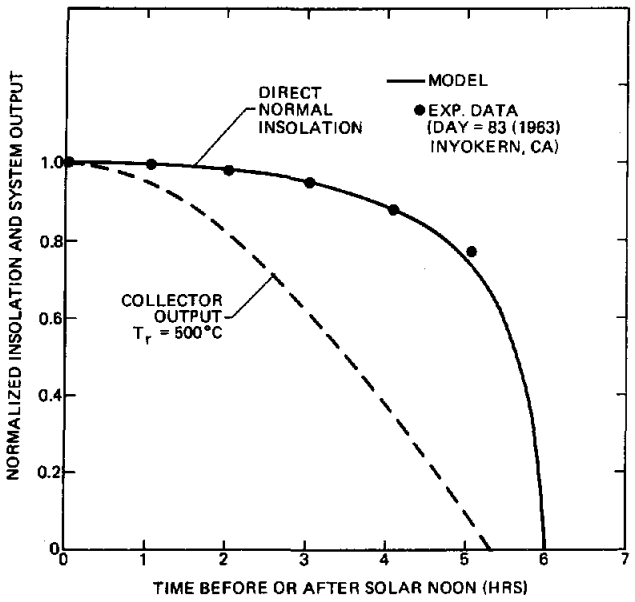

Fig. 7. Diurnal Variations in Direct Normal Insolation and Collector Output at Vernal Equinox

The influence of the emittance of the selective surface on the overall system daily efficiency is shown in Figure 8. The efficiency of the converter, the Carnot efficiency, dominates the overall system efficiency at low absorber temperatures. The influence of the emittance is readily discernible only above approximately 250°C. The influence of α/ϵ rapidly decreases as α/ϵ nears ten; the main gain has already been realized at α/ϵ of four. The contribution of the convective loss can be established by comparing the case of no convective and radiative losses, the dashed curve in Figure 8, with the case of no radiative loss, $\alpha/\epsilon = \infty$.

Figure 9 shows the influence of the nominal concentration ratio on the overall system daily efficiency. The change in the nominal concentration ratio could be a consequence of: a change in rim angle, a change in the nominal hemispherical concentration ratio, or a combination of changes in these two quantities (see Eq. (7)). A change in nominal hemispherical concentration ratio would stem from a desire to change the intercept factor γ, or it would be a consequence of changes in the tracking or mirror accuracy. Results are given in Figure 9 for nominal concentration ratios of 50, 100, and 150 for emittances of 0.22 and 0.9. An increase in nominal concentration ratio above 100 has an appreciable influence for the high emittance absorber;

however, a change from 100 to 150 results in less than a 2 percent increase in efficiency for absorber temperatures below 500°C with an absorber emittance of less than 0.22.

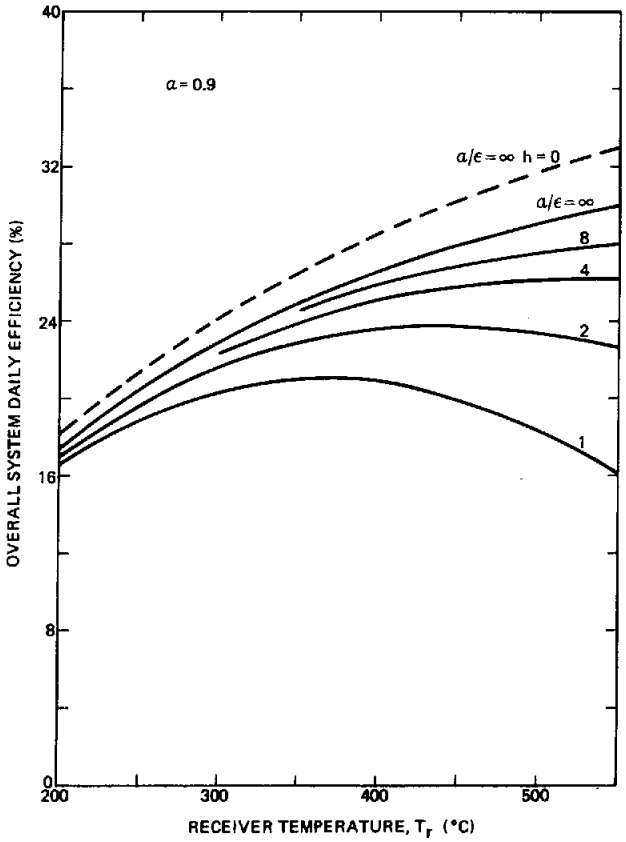

Fig. 8. The Influence of Radiative and Convective Heat Losses

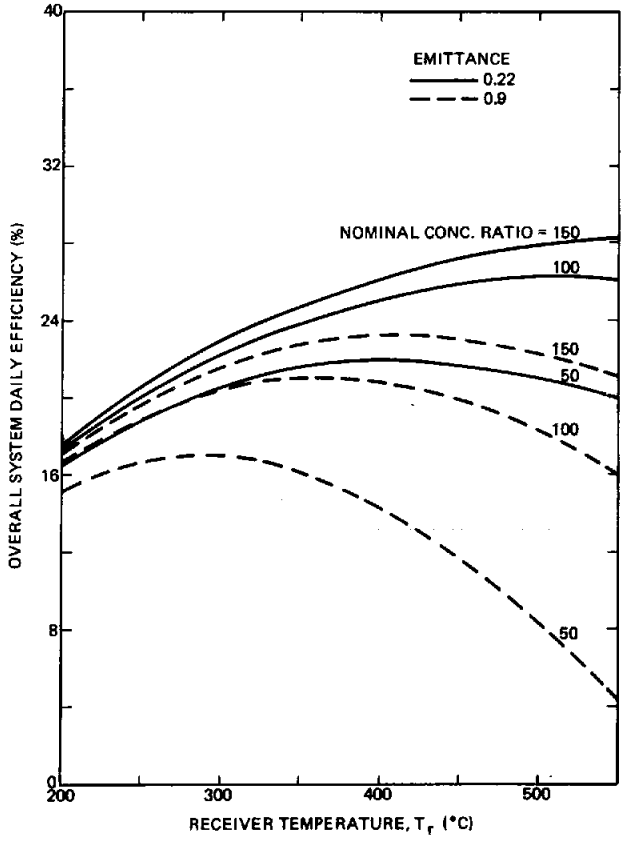

Fig. 9. Influence of Concentration Ratio on System Efficiency

The influence of the optical efficiency on the overall system daily efficiency is shown in Figure 10. Results are given for optical efficiencies of 1.0 (no optical losses), 0.8, 0.6, and 0.4. The influence of the optical efficiency is indeed strong. A change in η_0 of only 0.1 results in approximately a 4 percent change in the overall system daily efficiency for the range $1 \leq \eta_0 \leq 0.4$ and $300°C < T_r < 500°C$. Considering this strong influence of η_0, it appears that the increase in optical losses which result from the addition of a cover plate can probably not be offset by the consequential decrease in heat loss effected by the cover plate.

A breakdown of the Carnot, cosine, optical, and heat losses for receiver temperatures ranging from 200 to 700°C (392 to 1292°F) is shown in Figure 11. The cosine loss differs from the average daily cosine because the influence of the zenith angle on the attenuation of the direct normal insolation by the atmosphere is included. The second lowest curve given in Figure 11; i.e., the one obtained by excluding the Carnot loss, shows the efficiency of the collector system if it were to supply thermal energy.

A more comprehensive set of results is contained in Reference 6. Tabulated results are included in this reference which show the diurnal variation at winter solstice, vernal equinox, and summer solstice of: the sun's altitude angle, the sun's azimuth, the angle of incidence, the direct normal insolation, the heat flux through the aperture, the net heat flux through the receiver, the instantaneous power, the total power generated from time t before solar noon to time t after solar noon, the system total daily efficiency, several instantaneous efficiencies, and the instantaneous power per unit mirror area.

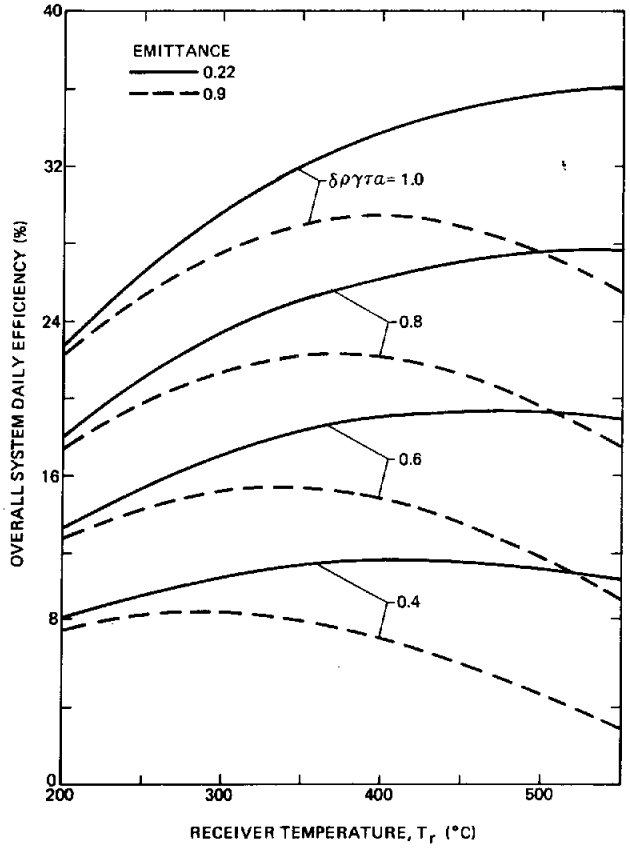

Fig. 10. Influence of Optical Losses on System Efficiency

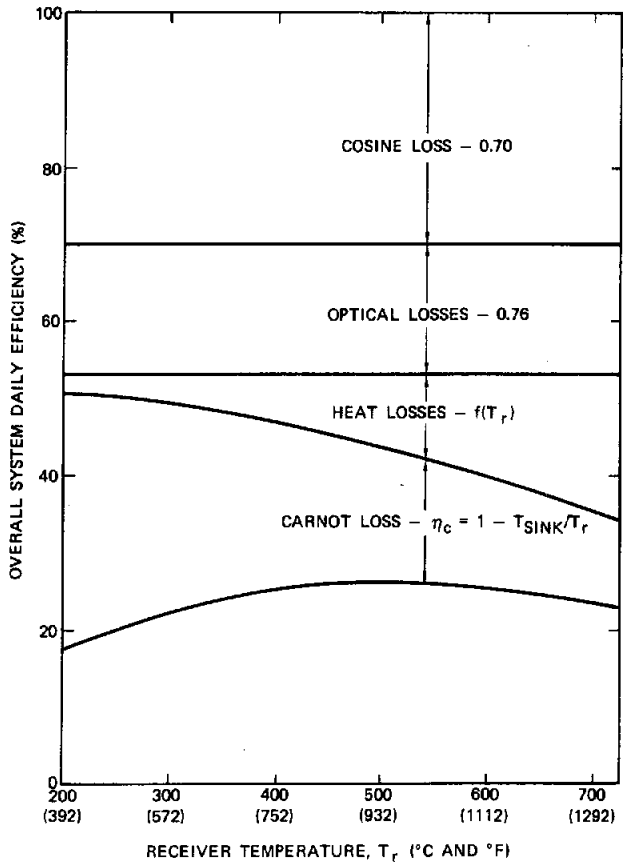

Fig. 11. Comparison of Cosine, Optical, Thermal, and Carnot Losses

Conclusions

It is difficult to predict the ultimate role to be played by the stationary reflector/tracking absorber solar collector. The penalty associated with the fixed reflector, the cosine loss, must be carefully weighed against the resulting advantages. The low effective concentration ratio of the SRTA collector, relative to tracking paraboloidal concentrators or the central receiver concept, results in relatively low efficiencies if the system is to be used for power generation. On the other hand, the complexity and cost of the two-axis tracking absorber limits the usefulness of the SRTA collector for solar heating and cooling applications in residences. Conclusions evident from the study are:

1. The winter performance of an SRTA collector with a horizontal aperture would generally not be acceptable at latitudes within the United States. The optimum slope of the collector for year-around, clear day performance is approximately equal to the latitude. A fixed aperture collector cannot effectively utilize long summer days; consequently, the average daily cosine for a fixed length day is not a strong function of the time of the year if the collector is sloped at an angle approximately equal to the latitude.

2. The cosine loss is appreciable even at the best time of the year.

3. The overall system performance is strongly dependent on the optical efficiency. The additional transmission loss associated with a cover plate, with energy incident at large angles, can probably not be offset by the reduction in heat losses which is effected by the cover plate.

4. Selective surfaces result in large improvements in performance. The increase in overall efficiency when the ratio of absorptance to emittance is increased from 1 to 4 is especially large.

5. The reduction in concentration ratio which results with rim angles less than 90° causes a significant degradation in collector efficiency which offsets to a large degree the benefit gained

by the decrease in the ratio of mirror area to aperture area. The results indicate that rim angles below approximately 60° will be unsatisfactory.

6. Large axial and circumferential variations occur in the energy distribution over the absorber. The energy distribution is dependent on both the time of the day and year. Hence the thermal design of an efficient absorber for the SRTA collector is a difficult task.

References

1. Steward, W. G., "A Concentrating Solar Energy System Employing a Stationary Spherical Mirror and Movable Collector," Proceedings of NSF/RANN Workshop on Solar Heating and Cooling for Buildings, Washington, D.C., 1973, pp. 24-25.

2. Steward, W. G. and Kreith, F., "Stationary Concentrating Reflector cum Tracking Absorber Solar Energy Collector: Optical Design Characteristics," Applied Optics, Vol. 14, No. 7, July 1975, pp. 1509-1512.

3. Kreider, J. F., "Thermal Performance Analysis of the Stationary Reflector/Tracking Absorber (SRTA) Solar Concentrator," ASME J. of Heat Transfer, Vol. 97, Series C, No. 3, August 1975, pp. 451-456.

4. The American Ephemeris and Nautical Almanac for the Year 1977, Nautical Almanac Office, U. S. Naval Observatory, U. S. Government Printing Office, Washington, 1975.

5. American Society of Heating, Refrigerating, and Air Conditioning, "Procedure for Determining Heating and Cooling Loads for Computerized Energy Calculations," 1971, pp. 18-24.

6. Clausing, A.M., Potential of a Solar Collector with a Stationary Spherical Reflector and a Tracking Absorber for Electrical Power Production, Sandia Laboratories Technical Report, SAND76-8039, August 1976.

UNLIMITED RELEASE

INITIAL DISTRIBUTION:

T. B. Cook, 8000; Attn: C. H. DeSelm, 8200
B. F. Murphey, 8300
W. C. Scrivner, 8400
L. Gutierrez, 8100; Attn: C. S. Selvage, 8180
A. C. Skinrood, 8184 (50)
A. M. Clausing, 8184 (50)
Technical Publications and Art Division, 8265, for TIC (2)
F. J. Cupps, 8265/Technical Library Processes Division, 3141
Technical Library Processes Division, 3141 (4)
Library and Security Classification Division, 8266 (5)